Defect Modes in Multilayered Piezoelectric Structures

D. G. Piliposyan

Abstract—Propagation of electro-elastic waves in a piezoelectric waveguide with finite stacks and a defect layer is studied using a modified transfer matrix method. The dispersion equation for a periodic structure consisting of unit cells made up from two piezoelectric materials with metallized interfaces is obtained. An analytical expression, for the transmission coefficient for a waveguide with finite stacks and a defect layer, that is found can be used to accurately detect and control the position of the passband within a stopband. The result can be instrumental in constructing a tunable waveguide made of layers of different or identical piezoelectric crystals and separated by metallized interfaces.

Keywords—Defect mode, Bloch waves, periodic phononic crystal, piezoelectric composite waveguide.

I. INTRODUCTION

ELECTRO-MECHANICAL coupling in piezoelectric materials significantly changes the properties of acoustic waves in periodic structures and reveals new properties compared to those of purely elastic crystals. These properties have been studied in one, two and three dimensional piezoelectric periodic structures [1]-[7].

Due to the electro-mechanical coupling, piezoelectric phononic crystals become sensitive to the electric properties of the interfaces, here again exhibiting new and distinctive acoustic effects [8], [9]. Reflection spectra of electro-elastic waves in periodic structures consisting of transverse isotropic piezoelectric layers with interfaces covered by thin metallized coatings was theoretically investigated in [10], [11].

Bloch waves in piezoelectric periodic waveguides suggest even richer underlying physics than in layered optical waveguides and hence their properties are of particular interest [12]. Identification of band gaps, frequencies of possible standing waves, trapped modes, and slow waves in periodic piezoelectric waveguides can lead to advances in imaging devices, delay line device technologies, and the prevention and filtering of unwanted vibrations. Trapping waves due to thickness variations and mechanisms of slow waves near cut-off frequencies in an elastic waveguide have been investigated in [13], [14]. Using matrix methods, these problems in in-plane and out-of-plane elasticity for waves in periodic waveguides have been studied in [15], [16].

Piezoelectric periodic waveguides with full contact interfacial conditions have been discussed in [17]-[19]. Electrically shorted interfaces however cannot be obtained from full contact interfacial conditions as a particular case since the amplitudes at interfaces become connected via degenerate matrices which cannot be inverted. Therefore, this has to be investigated as a separate problem. When there is not a full interfacial contact, for example electrically shorted or magnetically shorted interfaces between layers, the wave process is described by only one dispersion relation as oppose to two for full contact interfaces [7]. In this case, only one coupled electro-elastic wave propagates in the system combining both elastic and electro-magnetic effects.

In this paper, the problem of elastic wave propagation in periodic waveguides is solved by a modal decomposition approach based on eigenfunction expansion of the elastic displacements, stresses, magnetic and electric fields, where the eigenfunctions are the orthogonal wave-field modes of an infinite homogeneous waveguide [17]. Using the Sylvester theorem for unimodular matrices [20], an analytical expression for reflection transmission coefficients is found. It is further shown that, if the number of layers in the waveguide is large enough, the reflection coefficient reaches a value close to unity when the resonant conditions of the Bragg type are satisfied (i.e., when the value of the wave number lies inside the forbidden zones of the Bloch spectrum).

In order to control the frequency band structure, including the location and bandwidth of stopbands, tunable periodic structures can be designed by introducing defect layers into the structure, changing the geometry and altering the elastic characteristics of these inclusions [21], [22]. In this paper, we propose a novel tunable phononic waveguide with a defect mode made by inserting a dielectric layer into a piezoelectric waveguide with metalized interfaces. An analytical formula for the reflection/transmission coefficient which is found can be used to develop a tunable phononic waveguide.

II. THE STATEMENT OF THE PROBLEM AND MODAL EXPANSION

In this section, we obtain an analytical expression for the dispersion equation for electro-magneto-elastic coupled shear (SH) waves propagating along a finite-width periodic waveguide without the defect layer. The unit cell has length β and occupies a region $-\infty < x < \infty, -\infty < z < \infty, 0 < y < h$. Each cell is made of two different hexagonal piezoelectric materials: (1) of length a_1 and (2) of length a_2 ($\beta = a_1 + a_2$) with crystallographic axes directed along the Oz direction (Fig. 1).

D G Piliposyan is with the Department of Dynamics of Deformable Systems and Coupled Fields, Institute of Mechanics, 375024 Bagramyan ave., Yerevan, Armenia (e-mail: piliposyan@mechins.sci.am).
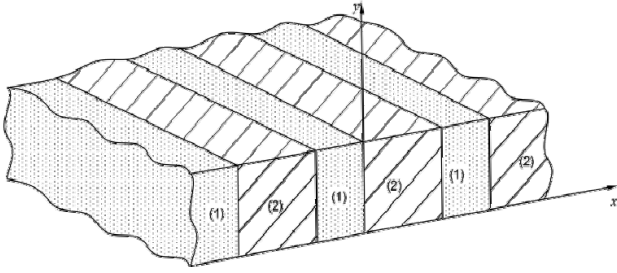
Fig. 1 Periodic waveguide with a unit cell made of two piezoelectric media

The interconnected elastic and electro-magnetic excitations are described by the equations and constitutive relations (1)-(3) [8].

$$\frac{\partial \sigma_{ik}}{\partial x_k} = \rho \frac{\partial^2 u_i}{\partial t^2} \tag{1}$$

$$\nabla \times \mathbf{E} = -\frac{\partial \mathbf{B}}{\partial t}, \nabla \times \mathbf{H} = \frac{\partial \mathbf{D}}{\partial t} \tag{2}$$

$$\sigma_{ij} = c_{ijkl}s_{kl} - e_{kij}E_k, \ D_i = e_{ijk}s_{jk} + \varepsilon_{ij}E_j, \tag{3}$$

where σ_{ik} is the stress tensor, ρ is the mass density, u_i is the displacement vector field, D_i and E_i are components of the electric displacement and electric field intensity, $\mathbf{B}$ and $\mathbf{H}$ are the magnetic field induction and intensity vectors, respectively. In constitutive relations (3), c_{ijkl} is the stiffness tensor, e_{ijk} and s_{kl} are the piezoelectric and strain tensors, and ε_{ij} is the dielectric permittivity matrix.

Harmonic time dependence, $\exp(i\omega t)$ for all the physical variables with ω as wave angular frequency is assumed henceforth. We assume that waves propagate in the (x,y) plane. Taking notations $H_z = i\omega H$, $u_z = u$ the system of equations (1)-(3) can be reduced to the uncoupled system of equations (4), (5)

$$\frac{\partial^2 u(x,y)}{\partial x^2} + \frac{\partial^2 u(x,y)}{\partial y^2} + \omega^2 \frac{\rho}{G} u(x,y) = 0 \tag{4}$$

$$\frac{\partial^2 H(x,y)}{\partial x^2} + \frac{\partial^2 H(x,y)}{\partial y^2} + \omega^2 \varepsilon_{11}\mu_{33} H(x,y) = 0 \tag{5}$$

and constitutive relations expressed via $H(x,y)$ and $u(x,y)$

$$E_y = -\frac{e_{15}}{\varepsilon_{11}} \frac{\partial u_z}{\partial y} + \frac{1}{\varepsilon_{11}} \frac{\partial H}{\partial x}, \ E_x = -\frac{e_{15}}{\varepsilon_{11}} \frac{\partial u}{\partial x} - \frac{1}{\varepsilon_{11}} \frac{\partial H}{\partial y}, \tag{6}$$

$$\sigma_{xz} = G\frac{\partial u}{\partial x} + \frac{e_{15}}{\varepsilon_{11}} \frac{\partial H}{\partial y}, \ \sigma_{yz} = G\frac{\partial u}{\partial y} - \frac{e_{15}}{\varepsilon_{11}} \frac{\partial H}{\partial x}, \tag{7}$$

where $G = c_{44} + e_{15}^2/\varepsilon_{11}$. Dimensionless coordinates $x = \tilde{x}h$ and $y = \tilde{y}h$ will be introduced and the tilde sign will be omitted henceforth. Two types of boundary conditions on the waveguide walls will be considered:

1) Displacement-clamped and electrically-shorted

$$u(x,0) = 0, \ E_x(x,0) = 0, \ u(x,1) = 0, \ E_x(x,1) = 0. \tag{8}$$

2) Traction free and magnetically-closed

$$H(x,0) = 0, \ \sigma_{yz}(x,0) = 0, \ H(x,1) = 0, \ \sigma_{yz}(x,1) = 0. \tag{9}$$

The solution of (4)-(5) can be written as $(u(x,y), H(x,y)) = (u(y), H(y))(e^{iqx}, e^{isx})$ leading to an eigenvalue problem with discrete eigenvalues q_n and s_n, and corresponding mode solutions $(u_n(x,y), H_n(x,y))$ with

$$u_n(x,y) = a_n(x)r_n(y), \ H_n(x,y) = ec_n(x)z_n(y), \tag{10}$$

$$E_{yn}(x,y) = \eta v_n(x)z_n(y), \ \sigma_{xzn}(x,y) = Gw_n(x)r_n(y), \tag{11}$$

$$r_n(y) = \begin{cases} \sin(p_n y) \\ \cos(p_n y) \end{cases}, \quad z_n(y) = \begin{cases} \cos(p_n y) \\ \sin(p_n y) \end{cases}, \tag{12}$$

where $e = e_{15}$ and is included in the expression of $H_n(x,y)$ to harmonise the dimensions of all the wave-field functions and

$$\begin{aligned} w_n(x) &= \left[q_n b_n(x) + (-1)^i \theta p_n c_n(x) \right], \\ v_n(x) &= \left[(-1)^i p_n a_n(x) + s_n d_n(x) \right], i = 1, 2 \end{aligned} \tag{13}$$

$$\eta = \frac{e}{\varepsilon}, \ \theta = \frac{e^2}{G\varepsilon}, \ q_n = \sqrt{\frac{\omega^2 h^2}{c_0^2} - p_n^2}, \ s_n = \sqrt{\frac{\omega^2 h^2}{c^2} - p_n^2},$$

$$c_0 = \sqrt{\frac{G}{\rho}}, c = \sqrt{\frac{1}{\mu\varepsilon}}, \tag{14}$$

c_0 is the velocity of the transverse wave in the medium, c is the speed of the electromagnetic wave, $i = 1, 2$ correspond to the upper and lower terms in (12) with $p_n = \pi n$ and $p_n = \pi(n-1)$, $n = 0, 1, 2\ldots$ respectively, corresponding to solutions for boundary conditions (8) and (9), and the notations (15) are introduced within a homogeneous material [17].

$$a_n(x) = A_n \exp(iq_n x) + B_n \exp(-iq_n x), b_n(x) = i(A_n \exp(iq_n x) - B_n \exp(-iq_n x)),$$
$$c_n(x) = C_n \exp(is_n x) + D_n \exp(-is_n x), d_n(x) = i(C_n \exp(is_n x) - D_n \exp(-is_n x)), \quad (15)$$

where $A_n \exp(iq_n x)$ and $C_n \exp(is_n x)$ correspond to forward propagating, $B_n \exp(-iq_n x)$ and $D_n \exp(-is_n x)$ are the reflected waves, and A_n, B_n, C_n, D_n are constants.

A. Solution for a Periodic Piezoelectric Waveguide with Metallized Interfaces

The interface conditions between two different homogeneous materials are continuity conditions for the displacement and the normal stresses

$$\begin{pmatrix} u^{(1)}(x) \\ \sigma_{xz}^{(1)}(x) \end{pmatrix} = \begin{pmatrix} u^{(2)}(x) \\ \sigma_{xz}^{(2)}(x) \end{pmatrix} \quad (16)$$

and, since the layers are separated by thin metallized coatings, zero electrical field at both sides of the interfaces (Fig. 1).

$$E_y^{(1)}(x) = 0, \ E_y^{(2)}(x) = 0 \quad (17)$$

Using (11)-(13), the boundary conditions at the interfaces $x = 0$ and $x = a_1$ can be written as

$$\sum_n \begin{pmatrix} a_n^{(1)}(x) r_n^{(1)}(y) \\ G^{(1)} w_n^{(1)}(x) r_n^{(1)}(y) \end{pmatrix} = \sum_n \begin{pmatrix} a_n^{(2)}(x) r_n^{(2)}(y) \\ G^{(2)} w_n^{(2)}(x) r_n^{(2)}(y) \end{pmatrix} \quad (18)$$

$$v_n^{(1)}(x) = 0, \ v_n^{(2)}(x) = 0 \quad (19)$$

where the superscripts 1,2 indicate the first and second material, respectively.

An inner product can be defined as

$$\langle r_m(y) | r_n(y) \rangle = \int_0^h r_m(y) r_n(y) dy \quad (20)$$

which has an orthogonality feature within the same material. Taking the inner product of (18) with a single mode m gives

$$\begin{pmatrix} a_n^{(1)}(x) L_{nm} \\ w_n^{(1)}(x) L_{nm} \end{pmatrix} = \begin{pmatrix} a_m^{(2)}(x) I \\ \gamma w_n^{(2)}(x) I \end{pmatrix}, \quad (21)$$

where $L_{mn} = \int_0^1 r_n^{(1)}(y) r_m^{(2)}(y) dy$, ($n, m = 1, 2, 3 \dots$).

For electrically open boundary conditions at interfaces when the wave characteristics are continuous, the transfer matrix coupling the wave fields in neighboring cells can be constructed directly by joining the wave fields at the interfaces [7]. The transfer matrix in the case of electrically shorted boundary conditions (19) is not possible to construct since, in this case, the interface matrices are degenerate and impossible to invert. In this case, using (19), the amplitudes $c_n^{(i)}(x)$ and $d_n^{(i)}(x)$ can be eliminated from (21), and the transfer matrix can be modified and written in terms of the vectors $\mathbf{a}^{(j)} = \left[a_n^{(j)}(x) \right]_{n=1,2,\dots N}$ and $\mathbf{b}^{(j)} = \left[b_n^{(j)}(x) \right]_{n=1,2,\dots,N}$ in the following way:

$$N_1 \begin{pmatrix} \mathbf{a}^{(1)}(0) \\ \mathbf{b}^{(1)}(0) \end{pmatrix} = N_2 \begin{pmatrix} \mathbf{a}^{(2)}(0) \\ \mathbf{b}^{(2)}(0) \end{pmatrix}, R_1 \begin{pmatrix} \mathbf{a}^{(1)}(a_2) \\ \mathbf{b}^{(1)}(a_2) \end{pmatrix} = R_2 \begin{pmatrix} \mathbf{a}^{(2)}(a_2) \\ \mathbf{b}^{(2)}(a_2) \end{pmatrix} \quad (22)$$

with

$$N_1 = \begin{pmatrix} L, & 0 \\ LV^{(1)}, & LQ^{(1)} + LW^{(1)} \end{pmatrix}, N_2 = \begin{pmatrix} I, & 0 \\ -\gamma V^{(2)}, & \gamma Q^{(2)} + \gamma W^{(2)} \end{pmatrix},$$

$$R_1 = \begin{pmatrix} L, & 0 \\ -LV^{(1)}, & LQ^{(1)} + LW^{(1)} \end{pmatrix}, R_2 = \begin{pmatrix} I, & 0 \\ \gamma V^{(2)}, & \gamma Q^{(2)} + \gamma W^{(2)} \end{pmatrix} \quad (23)$$

where matrices $Q^{(j)}$, $V^{(j)}$ and $W^{(j)}$ have elements

$$V_{mn}^{(j)} = \left(p_n^{(j)} \right)^2 \frac{\theta^{(j)} \left(\cos\left(a_j s_n^{(j)} \right) - \cos\left(a_j q_n^{(j)} \right) \right)}{s_n^{(j)} \sin(a_j s_n^{(j)})} \delta_{mn},$$

$$W_{mn}^{(j)} = \left(\left(p_n^{(j)} \right)^2 \frac{\theta^{(j)}}{s_n^{(j)}} \frac{\sin(a_j q_n^{(j)})}{\sin(a_j s_n^{(j)})} \right) \delta_{mn}, \quad (24)$$

$$Q_{mn}^{(j)} = q_n^{(j)} \delta_{nm}, \ \gamma = \frac{G_2}{G_1}$$

and I is an identity matrix, and δ_{mn} is the Kronecker delta operator.

Writing the Bloch-Floquet conditions as

$$\exp(ik\beta) \left(\mathbf{a}^{(1)}(-a_1), \mathbf{b}^{(1)}(-a_1) \right)^T = \left(\mathbf{a}^{(1)}(a_2), \mathbf{b}^{(1)}(a_2) \right)^T$$

where k is the Bloch wave number, and using the transfer matrices (23) across the interfaces, the problem can be written in the following form (25)

$$\exp(ik\beta) \begin{pmatrix} \mathbf{a}^{(1)}(-a_1) \\ \mathbf{b}^{(1)}(-a_1) \end{pmatrix} = \left(R_1^{-1} R_2 \right) T^{(2)}(0) \left(N_2^{-1} N_1 \right) T^{(1)}(-a_1) \begin{pmatrix} \mathbf{a}^{(1)}(-a_1) \\ \mathbf{b}^{(1)}(-a_1) \end{pmatrix} \quad (25)$$

where

$$T^{(j)}(x') = \begin{pmatrix} C_{q_n}^{(j)} & S_{q_n}^{(j)} \\ -S_{q_n}^{(j)} & C_{q_n}^{(j)} \end{pmatrix} \quad (26)$$

is the transfer matrix within a homogeneous material, and $C_{q_n}^{(j)}$ and $S_{q_n}^{(j)}$ are $N \times N$ matrices with entries $\cos(q_n^{(j)}(x'-x))$ and $\sin(q_n^{(j)}(x'-x))$ along the main diagonals.

For homogeneous boundary conditions on the guide walls, the matrix L in (23) becomes an identity matrix, the propagating modes are separated from each other, and each gives rise to the dispersion equation [8] by (27)

$$\cos(k\beta) = -\frac{f(p,\omega)}{g(p,\omega)}, \qquad (27)$$

$$f(p,\omega) = A + Q_1 Q_2 P + Q_1 R_1 + Q_2 R_2, \quad g(p,\omega) = (1+Q_1)(1+Q_2),$$

where

$$R_{1,2} = \cos\left(a_{1,2}q^{(1,2)}\right)\cos\left(a_{2,1}s^{(2,1)}\right)$$

$$+ \frac{e^{(2,1)^2}\varepsilon^{(1,2)}q^{(1,2)}}{e^{(1,2)^2}\varepsilon^{(2,1)}q^{(2,1)}}\frac{\sin\left(a_{1,2}q^{(1,2)}\right)}{\sin\left(a_{2,1}q^{(2,1)}\right)}\left(\cos\left(a_{2,1}q^{(2,1)}\right)\cos\left(a_{1,2}s^{(1,2)}\right)-1\right),$$

$$A = \cos\left(a_1 q^{(1)}\right)\cos\left(a_2 q^{(2)}\right)$$

$$- \frac{(G^{(1)^2}q^{(1)^2} + G^{(2)^2}q^{(2)^2})}{2q^{(1)}q^{(2)}G^{(1)}G^{(2)}}\sin\left(a_1 q^{(1)}\right)\sin\left(a_2 q^{(2)}\right),$$

$$Q_{1,2} = \frac{p^2 e^{(1,2)^2}\sin\left(a_{1,2}s^{(1,2)}\right)}{G^{(1,2)}\varepsilon^{(1,2)}q^{(1,2)}s^{(1,2)}\sin\left(a_{1,2}q^{(1,2)}\right)},$$

$$e^{(j)} = e_{12}^{(j)}, \quad \varepsilon^{(j)} = \varepsilon_{11}^{(j)}, \quad \mu^{(j)} = \mu_{33}^{(j)}, \qquad j = 1,2.$$

Without the piezoelectric effect, (27) will describe the propagation of the acoustic wave in the periodic waveguide with the dispersion equation $\cos(k\beta) = A$.

Dispersion equation (27) is the same both for displacement-clamped and electrically-shorted (8), and traction free and magnetically-closed boundary conditions (9) on the waveguide walls. In the case of boundary condition (8), mode $n=0$ leads to a trivial solution for the displacement and electromagnetic field independent of y, $H(x,y) = H(x)$ which due to electrically shorted interface conditions leads to no wave propagation. In the case of boundary condition (9) mode, $n=0$ leads to a solution for the displacement that is independent of y, $u(x,y) = u(x)$, and a trivial solution for the electromagnetic field function, giving the propagation only of an acoustic wave described by the dispersion equation $\cos(\beta k) = A$ with the piezoelectric effect present only in the piezoelectrically stiffened elastic modulus G.

For a superlattice with cells composed of two identical piezoelectric materials ($e_1 = e$, $e_2 = e$) of equal widths $a_2 = a_1 = a$, the dispersion equation (27) takes the form (28):

$$\cos(ak) = \frac{\cos(aq)\sin(as) + \eta\cos(as)\sin(aq)}{\sin(as) + \eta\sin(aq)}, \eta = \frac{\theta p^2}{qs}, (28)$$

where the parameters q and s are expressed by (14) without indices. It is clear from (28) that, for electrically shorted interfaces between two constituent materials in the waveguide, band gaps are possible if these materials are identical. In this case, however, the opposite polarization will not affect the band structure.

III. REFLECTION/TRANSMISSION OF ACOUSTIC WAVES IN A PIEZOELECTRIC WAVEGUIDE WITH FINITE STACKS

In this section, we investigate the reflection/transmission properties of a finite stack of cells in a piezoelectric waveguide by coupling the wave fields in neighboring layers via a matrix propagator. We consider a structure consisting of a stack of M cells, each containing a pair of layers a_j, $j=1,2$ made from different piezoelectric crystals and one additional single layer, thus $2M+1$ layers altogether (Fig. 1). On each side the waveguide has two infinite piezoelectric substrates made from material 2.

From (4)-(7), the complete magneto-elastic wave field in the mth cell is

$$\begin{pmatrix} u_{(m)}(x) \\ \sigma_{xz(m)}(x) \\ H_{(m)}(x) \\ E_{y(m)}(x) \end{pmatrix} = A\begin{pmatrix} 1 \\ iGq \\ 0 \\ ep/\varepsilon \end{pmatrix}e^{iq(x-m\beta)} + B\begin{pmatrix} 1 \\ -iGq \\ 0 \\ ep/\varepsilon \end{pmatrix}e^{-iq(x-m\beta)}$$

$$+ C\begin{pmatrix} 0 \\ -e^2 p/\varepsilon \\ 1 \\ -ie^2 s/\varepsilon \end{pmatrix}e^{is(x-m\beta)} + D\begin{pmatrix} 0 \\ -e^2 p/\varepsilon \\ 1 \\ ie^2 s/\varepsilon \end{pmatrix}e^{-is(x-m\beta)}, \qquad (29)$$

where the factor $\exp(i(py - \omega t))$ is omitted, and all the parameters apart from p have superscripts (j) which are also omitted, ($j=1,2$) correspond to the material number in the unit cell. We will investigate the transmission properties of only acoustic waves since the piezoelectric effect does not have a noticeable effect on electromagnetic waves. From (29) and (17), the amplitudes $C^{(j)}$ and $D^{(j)}$ in the expression for $E_y^{(j)}$ can be expressed via the amplitudes $A^{(j)}$ and $B^{(j)}$

$$\begin{pmatrix} C^{(1)} \\ D^{(1)} \end{pmatrix} = \begin{pmatrix} \eta_+^{(1)}e^{ia_1(s^{(1)}-q^{(1)})} & \eta_-^{(1)}e^{ia_1(s^{(1)}+q^{(1)})} \\ -\eta_-^{(1)} & -\eta_+^{(1)} \end{pmatrix}\begin{pmatrix} A^{(1)} \\ B^{(1)} \end{pmatrix},$$

$$\begin{pmatrix} C^{(2)} \\ D^{(2)} \end{pmatrix} = \begin{pmatrix} \eta_+^{(2)}e^{i\beta(s^{(2)}-q^{(1)})} & \eta_-^{(2)}e^{i\beta(s^{(2)}+q^{(1)})} \\ -\eta_-^{(2)}e^{-ia_1(s^{(1)}+q^{(1)})} & -\eta_+^{(2)}e^{-ia_1(s^{(2)}-q^{(1)})} \end{pmatrix}\begin{pmatrix} A^{(2)} \\ B^{(2)} \end{pmatrix} \quad (30)$$

$$\eta_\pm^{(j)} = \frac{ip(1-e^{ia_j(s^{(j)}\pm q^{(j)})})}{s^{(j)}(e^{2ia_j s^{(j)}}-1)}$$

The amplitudes $C^{(j)}$ and $D^{(j)}$ will be eliminated by substituting (30) into the expression for $\sigma_{xz}^{(j)}(x)$ in the boundary conditions (16). Formula (16) will have only the incident and reflected amplitudes $A^{(j)}$ and $B^{(j)}$ of a coupled magneto-elastic wave. Then, a 2×2 unimodular transfer matrix S coupling the amplitudes of forward and backward

travelling waves $A_m^{(1)}$ and $B_m^{(1)}$ in a_1 layers of the two neighbouring cells (m) and ($m+1$) can be constructed such that

$$\begin{pmatrix} A_m^{(1)} \\ B_m^{(1)} \end{pmatrix} = S \begin{pmatrix} A_{m+1}^{(1)} \\ B_{m+1}^{(1)} \end{pmatrix} \qquad (31)$$

where $S = S^{(1)} S^{(2)}$, the elements of matrices $S^{(1)}$ and $S^{(2)}$ are

$$S_{11}^{(1)} = S_{22}^{(1)*} = e^{-i\beta q^{(2)}} \frac{(\psi_+^{(1)} - 1) + \gamma(\psi_+^{(2)} - 1)}{\psi_+^{(1)} - \psi_-^{(1)} - 2},$$

$$S_{12}^{(1)} = S_{21}^{(1)*} = e^{i\beta q^{(2)}} \frac{(\psi_+^{(1)} - 1) + \gamma(\psi_2^{(2)} + 1)}{\psi_+^{(1)} - \psi_-^{(1)} - 2}, \qquad (32)$$

$$S_{11}^{(2)} = S_{22}^{(2)*} = e^{-ia_1(q^{(1)} - q^{(2)})} \frac{(\psi_+^{(1)} - 1) + \gamma(\psi_+^{(2)} - 1)}{\gamma(\psi_+^{(2)} - \psi_-^{(2)} - 2)},$$

$$S_{12}^{(2)} = S_{21}^{(2)*} = e^{ia_1(q^{(1)} + q^{(2)})} \frac{(\psi_-^{(1)} + 1) + \gamma(\psi_+^{(2)} - 1)}{\gamma(\psi_+^{(2)} - \psi_-^{(2)} - 2)}, \qquad (33)$$

$$\psi_\pm^{(j)} = \chi^{(j)} \frac{1 - 2e^{ia_j(s^{(j)} \pm q^{(j)})} + e^{2ia_j s^{(j)}}}{e^{2ia_j s^{(j)}} - 1}, \quad \chi^{(j)} = \frac{p^2 \theta^{(j)}}{q^{(j)} s^{(j)}}, \quad (34)$$

and * in the superscript denotes the complex conjugate. The amplitudes of the incident A_I, reflected B_R and transmitted A_T acoustic waves in the two substrates will thus have the relation:

$$\begin{pmatrix} A_I \\ B_R \end{pmatrix} = S_I^{(2)} S^M S_T^{(1)} \begin{pmatrix} A_T \\ 0 \end{pmatrix} \qquad (35)$$

Here, $S_I^{(2)}$ is the transfer matrix of the bulk waves at the interface between the front substrate (made from material a_2) and the a_1 layer, and $S_T^{(1)}$ is the transfer matrix at the interface between the a_1 layer and the end substrate (made from material a_2). Hence, the elements of both matrices $S_I^{(2)}$ and $S_T^{(1)}$ can be obtained from the corresponding elements of the matrices $S^{(2)}$ and $S^{(1)}$ by taking the limit $a_2 \to \infty$. At acoustic frequencies, $s^{(j)}$ is always imaginary and writing $s^{(j)} = i\sqrt{p^2 - \omega^2 h^2 / c^{(j)2}} \approx ip$, ($j$=1,2) in (34) $\psi_2^{\pm}$ can be written as

$$\psi_\pm^{(2)} = i\chi_*^{(2)} \left(\frac{e^{\pm ia_2 q^{(2)}}}{\sinh a_2 p} - \coth a_2 p \right), \quad \chi_*^{(2)} = \frac{p\theta^{(2)}}{q^{(2)}}. \qquad (36)$$

As $a_2 \to \infty$, only the term $\psi_\pm^{(2)}$ in (34) will be affected, becoming in the limit $\psi_\pm^{(2)} = -i\chi^{(2)}$. On the other hand,

following [10], for the matrices $S^{(2)}$ and $S^{(1)}$ the approximation $\psi_\pm^{(2)} \approx -i\chi^{(2)}$ can be made at acoustic frequencies. Thus, with a good accuracy, we can assume that

$$S_I^{(2)} \approx S^{(2)}, \; S_T^{(1)} \approx S^{(1)}. \qquad (37)$$

The transfer matrix can be rewritten as

$$S_I^{(2)} S^M S_T^{(1)} = \hat{S}^{M+1}, \qquad (38)$$

where

$$\hat{S} = S^{(2)} S^{(1)} \qquad (39)$$

is a unimodular transfer matrix connecting the amplitudes of incident and reflected waves in the a_2 layers of (m)th and ($m+1$)th cells

$$\begin{pmatrix} A_m^{(2)} \\ B_m^{(2)} \end{pmatrix} = \hat{S} \begin{pmatrix} A_{m+1}^{(2)} \\ B_{m+1}^{(2)} \end{pmatrix} \qquad (40)$$

Using the Sylvester's theorem for a 2×2 unimodular matrix, (38) can be written as (41)

$$\hat{S}^{M+1} = \begin{pmatrix} \hat{S}_{11} & \hat{S}_{12} \\ \hat{S}_{12}^* & \hat{S}_{11}^* \end{pmatrix}^{M+1} = \begin{pmatrix} \hat{S}_{11} U_M - U_{M-1} & \hat{S}_{12} U_M \\ \hat{S}_{12}^* U_M & \hat{S}_{11}^* U_N - U_{M-1} \end{pmatrix} \quad (41)$$

where $U_M = \dfrac{\sin((M+1)k\beta)}{\sin(k\beta)}$ and where the Bloch wave number k is defined by

$$\cos(k\beta) = (\hat{S}_{11} + \hat{S}_{11}^*) / 2. \qquad (42)$$

From (35), (37) and (41), the reflection/transmission problem can be written as

$$\begin{pmatrix} A_I \\ B_R \end{pmatrix} = \begin{pmatrix} \hat{S}_{11} U_M - U_{M-1} & \hat{S}_{12} U_M \\ \hat{S}_{12}^* U_M & \hat{S}_{11}^* U_M - U_{M-1} \end{pmatrix} \begin{pmatrix} A_T \\ 0 \end{pmatrix}. \qquad (43)$$

From (43) we find that the reflection coefficient is

$$R = \frac{B_R}{A_I} = \frac{\hat{S}_{12}^* U_M}{\hat{S}_{11} U_M - U_{M-1}}, \qquad (44)$$

and

$$|R|^2 = \frac{|\hat{S}_{12}|^2}{|\hat{S}_{12}|^2 + (\sin(k\beta) / \sin((M+1)k\beta))^2}. \qquad (45)$$

At the band edges, where $k\beta = \pi n$, the reflectivity will be given by

$$|R|^2 = \frac{|\hat{S}_{12}|^2}{|\hat{S}_{12}|^2 + (1/(M+1))^2} , \qquad (46)$$

and the transmissivity by $|T|^2 = 1 - |R|^2$. Within the band gaps, where $k\beta$ is complex, $k\beta = \pi n + i\delta$, formula (45) takes the form (47)

$$|R|^2 = \frac{|\hat{S}_{12}|^2}{|\hat{S}_{12}|^2 + (\sinh(\delta)/\sinh((M+1)\delta))^2} . \qquad (47)$$

It follows from (47) that the reflection coefficient will approach unity as the number of cells increases and the total reflection regions will precisely coincide with the stopband for Bloch waves.

A. Transmissions Coefficient in the Piezoelectric Composite Waveguide with a Defect Layer

We now introduce a defect layer Z as shown in Fig. 2, such that the waveguide has a mirror symmetry about this layer.
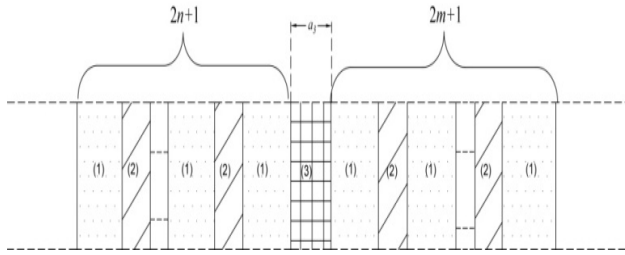

Fig. 2 Finite stack piezoelectric waveguide between two infinite substrates and a defect layer

The transfer matrix now will have the form of (48):

$$\begin{pmatrix} A_I \\ B_R \end{pmatrix} = \hat{S}^M Z \hat{S}^M \begin{pmatrix} A_T \\ 0 \end{pmatrix}, \qquad (48)$$

and Sylvester's theorem can be used to obtain an expression for the transmission coefficient

$$T = \frac{A_T}{A_I} = \frac{1}{Z_{11} U_{M-2}^2 - Z_2 U_{M-2} U_{M-1} + Z_3 U_{M-1}^2} , \qquad (49)$$

where $Z = \begin{pmatrix} Z_{11} & Z_{12} \\ Z_{12}^* & Z_{11}^* \end{pmatrix}$ is the transfer matrix through the defect layer and the following notations are introduced:

$$Z_2 = 2\hat{S}_{11} Z_{11} + \hat{S}_{12}^* Z_{12} + \hat{S}_{12} Z_{12}^*, \; Z_3 = |\hat{S}_{12}|^2 Z_{11}^* + \hat{S}_{11}\left(Z_2 - \hat{S}_{11} Z_{11}\right).$$

The analytical expression (49) for the transmission coefficient can be used to investigate the defect mode in a waveguide with a finite stack of cells, each cell composed of either two different or two identical piezoelectric elements.

IV. NUMERICAL RESULTS

Numerical calculations have been carried out for two piezoelectric phononic crystals. Material parameters of PZT-4 and BaTiO$_3$ have been used for one photonic crystal and PZT-4 for the piezoelectric waveguide with identical layers (Table I).

TABLE I
MATERIAL CONSTANTS OF PZT-4, LiIO$_3$ AND BaTiO$_3$

Material	Elastic constant $c_{44} \cdot 10^{10}$ N/m^2	Piezoelectric constant e_{15} C/m^2	Permittivity ε_{11} 10^{-11} F/m	Density ρ 10^3 kg/m^3
PZT-4	2.56	12.7	646	7.6
LiIO$_3$	1.78	0.89	6.434	3.402
BaTiO$_3$	5.43	11.6	1.744	6.02

Fig. 3 shows wave trapping for the lowest mode for a BaTiO$_3$ and LiIO$_3$ waveguide, where the horizontal lines show the cut-off frequencies in two materials. The nature of the trapping is the same as that described in detail in [17]. For a waveguide with short thin cells ($\beta < h$), the mode is localized near the interfaces between the two materials for all values of the reduced wave number (Fig. 3(a)). As the length of the unit cell increases compared to the waveguide height (Fig. 3(b)), the dispersion curves for the piezoelectric waveguide become flatter. Due to a large difference between the acoustic impedances of BaTiO$_3$ and LiIO$_3$, the frequency region of the piezoelectric waveguide with trapped waves is large and for longer cells includes several modes (Fig. 3(b)).
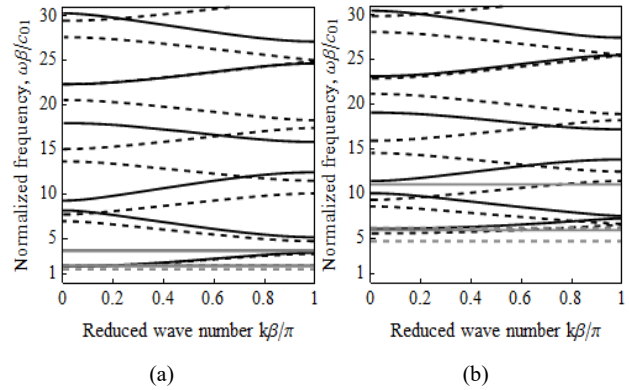

(a)   (b)

Fig. 3 Band structure for a LiIO$_3$ and BaTiO$_3$ piezoelectric phononic crystal for $n=1$ (a) β/h=0.5, (b) β/h=1.5. Solid lines and dashed lines show the band structure with and without the piezoelectric effect. Horizontal lines show the cut-off frequencies in the two materials

The transmission coefficients in Fig. 4 confirm the above results, showing full reflection when the Bragg resonance conditions are satisfied (i.e., when the value of the wave number lies inside the forbidden zones of the Bloch spectrum)

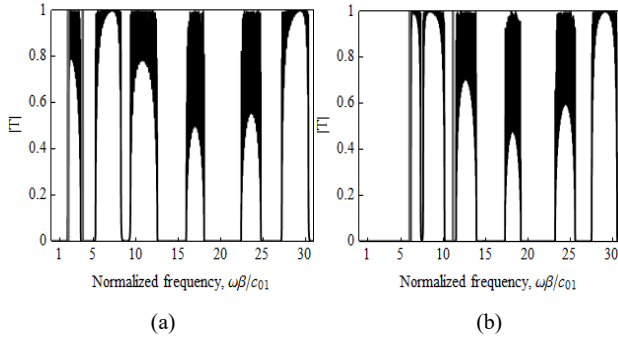and the number of layers is sufficiently large.

Fig. 4 Absolute value of the transmission coefficient for a LiIO$_3$ and BaTiO$_3$ piezoelectric phononic crystal for M=50 (a) β/h=0.5, (b) β/h=1.5. Vertical gray lines show the cut-off frequencies in each material

A superlattice made up of a unit cell with identical PZT-4 material also demonstrates frequency gaps and increasing cut-off frequencies for longer unit cells (Figs. 5 (a), (b)). The frequency gaps in this case are only in the middle of the Brillouin zone, where the first gap remains always the largest, and as can be seen also from the reflection coefficient (Fig. 6) does not have significant change in its width.
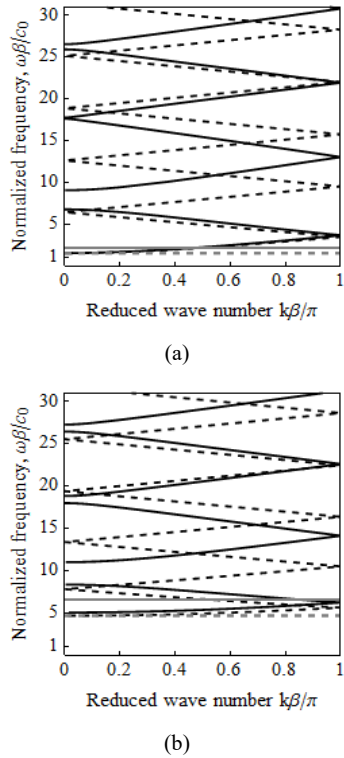

(a)

(b)

Fig. 5 Superlattice with identical PZT-4 crystals in both layers of the unit cell a) β/h=0.5, b) β/h=1.5. Dashed lines show the band structure without piezoelectric effect. Horizontal lines show the cut-off frequencies

Another interesting feature here is that the Bloch wave number can have a real value below the cut-off frequency. This is better shown for longer unit cells (Fig. 5(b)) and does not happen when the piezoelectric effect is neglected. This can also be shown analytically from the dispersion equation (28) where below cut-off acoustic frequencies $\omega^2/c_0{}^2 - p^2 < 0$ and $\omega^2/c^2 - p^2 < 0$. If we expand the right-hand side of (28) as a series with respect to a small parameter θ, the first term of series is $F(\omega) = \cos(aq) + \theta \dfrac{p^2}{qs} \dfrac{\sin(aq)}{\sin(as)} \left(\cos(as) - \cos(aq) \right)$.

Since $F(0) = \cosh(\pi\beta/h) > 1$, it follows that there is not propagating mode. At the cut-off frequency $\omega_0 = c_0 p/h$, taking into account that $(c_0/c)^2 \geq 1$, $F(\omega_0)$ can be approximated as $1 - \theta a_0 \pi \tanh(a_0\pi/2) < 1$. This means that there exists a region below the cut-off frequency where the waveguide supports an evanescent mode.
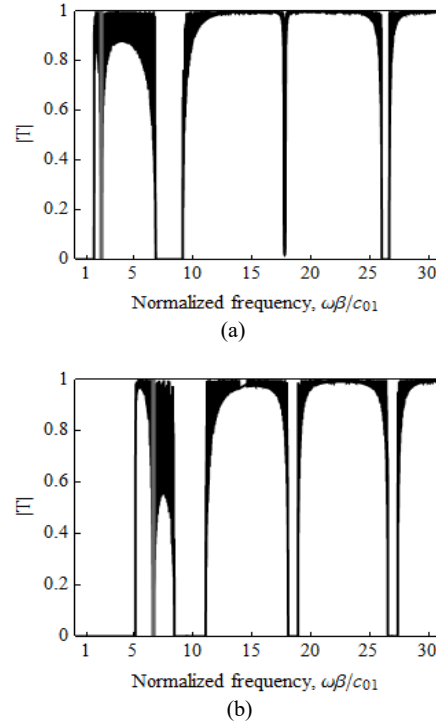

(a)

(b)

Fig. 6 Absolute value of the transmission coefficient, identical pzt-4 crystals in both layers of the unit cell, M=100, (a) β/h=0.5, (b) β/h=1.5. Vertical gray lines show the cut-off frequency

Due to the fixed electro-potential condition, a superlattice with identical elements in the unit cell demonstrates a much sharper resonant enhancement of transmission (Fig. 6). Since each interface in this case provides a reflection proportional to only the electromechanical coupling parameter $\theta < 1$ [10], near the Bragg resonance, where $|T| = 0$ for a sufficiently large number of layers, the transmission coefficient experiences a sharp decrease compared to waveguides with a unit cell made of different piezoelectric materials (Fig. 4).

V. Tunable Passband in the Piezoelectric Composite Waveguide

We now use the transmission coefficient (45) to investigate the transmission properties of SH waves in the piezoelectric waveguide with a defect layer (Fig. 2).

Fig. 7 compares the transmission spectrum of the piezoelectric composite waveguide $LiIO_3$ and $BaTiO_3$ with and without a defect layer. Without a defect layer (Fig. 7 (a)), a typical propagation feature with an acoustic bandgap is observed. The presence of a defect layer (Figs. 7 (b) and (c)) shows broadening of the forbidden band. Further, a passband with a transmission peak of 100% appears within the bandgap.

Increasing the thickness of the defect layer from $d_c = \beta$ (Fig. 7 (b)) to $d_c = 1.5\beta$ (Fig. 7 (c)) moves the passband from $\omega\beta/c_{01} = 8.7$ to $\omega\beta/c_{01} = 8.4$, demonstrating that the passband can be tuned by changing the thickness of the defect layer.
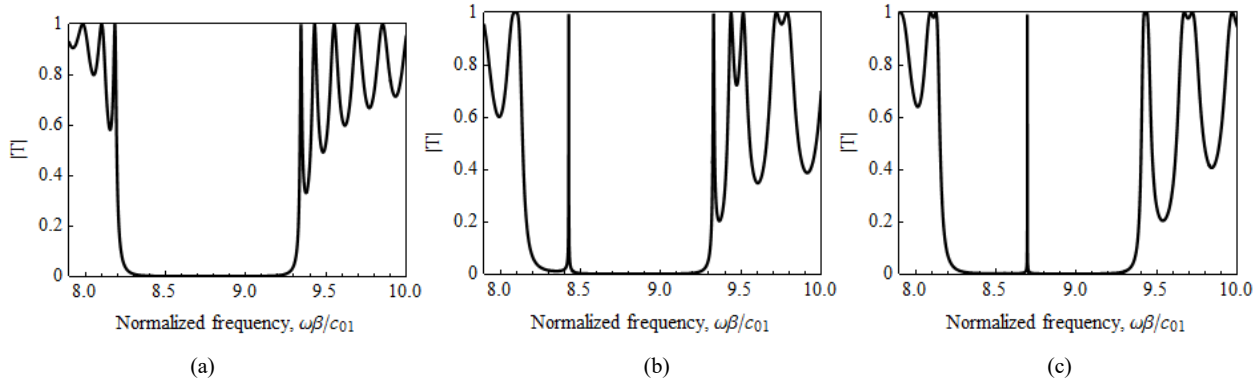

(a)　　　　　　　　　(b)　　　　　　　　　(c)

Fig. 7 Absolute values of the transmission coefficient for a $LiIO_3$ and $BatiO_3$ piezoelectric phononic crystal for $\beta/h=0.5$, $M=25$ (a) Without a defect layer, (b) With a defect layer thickness $d_c = \beta$, (c) With a defect layer thickness $d_c = 1.5\beta$
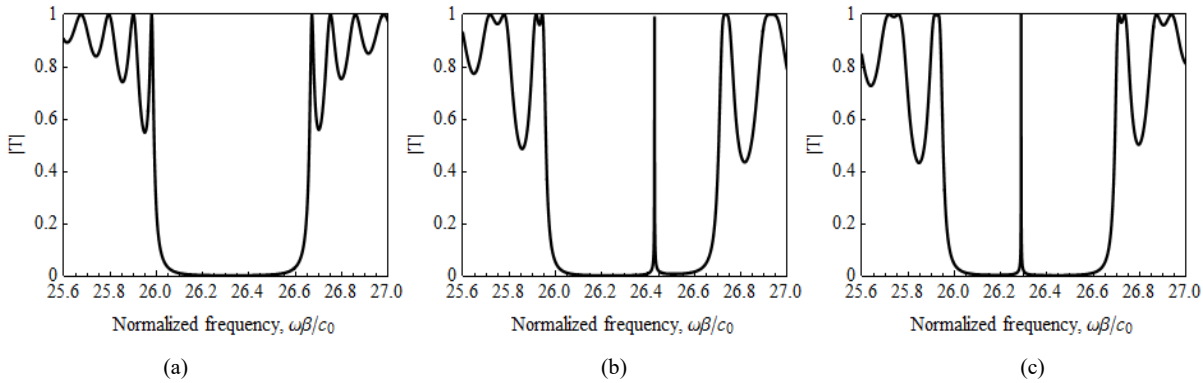

(a)　　　　　　　　　(b)　　　　　　　　　(c)

Fig. 8 Absolute values of the transmission coefficient, identical PZT-4 crystals in both layers of the unit cell for $\beta/h=0.5$, $M=25$, (a) Without a defect layer, (b) With a defect layer thickness $d_c = \beta$, (c) With a defect layer thickness $d_c = 1.5\beta$

Fig. 8 shows similar results for a piezoelectric waveguide with cells composed of an identical piezoelectric material PZT-4. The transmission spectrum for a waveguide without a defect layer is shown in Fig. 8 (a). Figs. 8 (b) and (c) show that the presence of a defect layer results in a slight broadening of the bandgap and the appearance of a 100% transmission passband within the bandgap. Changing the thickness of the defect layer from $d_c = \beta$ (Fig. 8 (b)) to $d_c = 1.5\beta$ (Fig. 8 (c)) moves the passband from $\omega\beta/c_{01} = 2.263$ to $\omega\beta/c_{01} = 2.262$ though in this case without changing the width of stop band.

VI. Conclusion

The propagation of elasto-electromagnetic coupled SH waves in a quasi-one dimensional periodic piezoelectric waveguide is considered within the full system of Maxwell's equations. Such a setting of the problem with perfectly matched physical fields at the interfaces allows the investigation of Bloch-Floquet waves in a wide range of frequencies including both acoustic and electromagnetic waves. The complete dispersion relation is described by two coupled equations and include information about a coupled elasto-electromagnetic wave and acousto-optic resonances called phonon-polariton. Without the piezoelectric effect the two equations decouple; one describes the propagation of an electromagnetic wave in a photonic crystal, and the other one expresses an acoustic wave in a phononic crystal.

In the case when there are not full interfacial contacts, the wave process is described by only one dispersion relation which in the absence of the piezoelectric effect describes the propagation of only one acoustic wave in a phononic crystal. In this case, only one coupled electro-elastic wave propagates in the system combining both elastic and electro-magnetic effects.

The structure of wave propagation strongly depends on the ratio of the length of the unit cell to the height of the waveguide β/h and differences between the elastic and electromagnetic properties of the piezoelectric layers.

When the unit cell in the waveguide is made from two different constituent materials, wave trapping occurs with the waves exponentially decaying in one layer, creating a stop band below the lowest of the two cut-off frequencies where no propagation is possible.

In the case of electrically shorted interface conditions band gaps exist also when the constituent materials in the cells of the waveguide are identical. In this case the periodic system becomes a periodic system of interfaces where the magnetic field intensity experiences discontinuity. There is only one cut-off frequency and instead of trapping there are evanescent modes propagating below the cut-off frequency. The reflection of an electro-elastic wave is caused by the equipotential condition on the interfaces. Since the parameter of electromechanical coupling is normally very small, the reflection coefficient experiences a sharp increase near the resonances providing sharpening of certain properties compared to periodic structure made from different piezoelectric layers with both metallised and non-metallized interfaces.

Controlling wave propagation properties including slowing down the propagation of light or sound or creating passband inside the stopband is also possible by introducing some disorder in periodically layered structures. We have found an analytical expression for the transmission coefficient that can be used to accurately detect the position of the passband inside a stopband. This can have applications in designing tunable waveguides which can even be made of layers of identical piezoelectric crystal separated by metallized interfaces.

REFERENCES

[1] A.K. Vashishth, V. Gupta, V., "Wave propagation in transversely isotropic porous piezoelectric materials", Int. J. Solids Struct. 46, 2009, pp. 3620–3632.
[2] Y.Z. Wang, F.M. Li, K. Kishimoto, Y.S. Wang, and W.H. Huang, "Wave band gaps in three-dimensional periodic piezoelectric structures", Mech. Research Comm. 36, 2009, pp. 461–468.
[3] M. Wilm, S. Ballandras, V. Laude, and T. Pastureaud, "A full 3D plane-wave expansion model for 1-3 piezoelectric composite structures", J. Acous. Soc.Amer. 112, 2002, pp. 943–952.
[4] X.Y. Zou, Q. Chen, B. Liang, and J.C. Cheng, "Control of the elastic wave band gaps in two-dimensional piezoelectric periodic structures", Sm. Mat. Struct. 17, 2008, p. 015008.
[5] Z.Z. Yan, Y.S. Wang, "Calculation of band structures for surface waves in two dimensional phononic crystals with a wavelet-based method", Phys. Rev. B 78, 2008, p. 094306.
[6] Y. Achaoui, A. Khelif, S. Benchabane, and V. Laude, "Polarisation state and level repulsion in two-dimensional phononic crystals and waveguides in the presence of material anisotropy", J. of Phys. D: Appll. Phys. 43, 2010, p. 185401.
[7] G.T. Piliposian, A.S. Avetisyan, and K.B. Ghazaryan, "Shear wave propagation in periodic phononic/photonic piezoelectric medium", Wave Motion 49(1), 2012, pp. 125-134.
[8] K.B. Ghazaryan, D.G. Piliposyan, "Interfacial effects for shear waves in one dimensional periodic piezoelectric structure", J. Sound Vib., 330(26), 2012, pp. 6456-6466.
[9] A.N. Darinskii, A.L. Shuvalov, O. Poncelet, A.A. Kutsenko, "Bulk longitudinal wave reflection/transmission in periodic piezoelectric structures with metallized interfaces", Ultrasonics, Volume 63, 2015, pp. 118-125.
[10] V.I. Alshits, A.L. Shuvalov, "Resonance reflection and transmission of shear elastic waves in multilayered piezoelectric structures", J. Appl. Phys. 77 (6), 1995, pp. 2659-2665.
[11] V.I. Alshits, A.S. Gorkunova, and A.L. Shuvalov, "Phase resonance in the reflection of acoustic waves by a system of piezocrystalline layers separated by cladding layers with screening properties", Zh. Eksp. Teor. Fiz. 110, 1996, pp. 924-937.
[12] A.L. Chen, Y.S. Wang, "Study on band gaps of elastic waves propagating in one dimensional disordered phononic crystals", Physica B 392, 2006, pp. 369–378.
[13] J. Postnova, R.V. Craster, R.V., "Trapped modes in topographically varying elastic waveguides", Wave Motion 44, 2007, pp. 205–221.
[14] R.V. Craster, S. Guenneau, and S.D.M. Adams, 2009, "Mechanism for slow waves near cut-off frequencies in periodic waveguides", Phys. Rev. B 79, 2009, p. 045129.
[15] S.D.M. Adams, R.V Craster, and S. Guenneau, "Bloch waves in periodic multi-layered acoustic waveguides", Proc. R. Soc. A 464, 2008, pp. 2669-2692.
[16] S.D.M.Adams, R.V Craster, and S. Guenneau, "Guided and standing Bloch waves in periodic elastic strips", Waves Rand. Compl. Media 19(2), 2009, pp. 321–346.
[17] D.G.Piliposyan, K.B. Ghazaryan, and G.T. Piliposian, "Shear Bloch waves and coupled phonon–polariton in periodic piezoelectric waveguides", Ultrasonics 54(2), 2014, pp. 644–654.
[18] M. Sugimoto, T. Makimoto, "Analysis of mode coupling in piezoelectric waveguides", Appl. Phys., 45(4), 1973, pp. 1643-1649.
[19] Y. Guo, W. Chen, and Y. Zhang, "Guided wave propagation in multi-layered piezoelectric structures", Sci. China Ser. G: Phys., Mech. &Astr. 52(7), 2009, pp. 1094-1104.
[20] A.A. Tovar, L.W. Casperson, "Generalized Sylvester theorem for periodic applications in matrix optics", J. Opt. Soc. Am. A, 12(3), 1995, pp. 578-590.
[21] C. Goffaux, J.P. Vigneron, "Theoretical study of a tunable phononic band gap system", Phys. Rev. B: Condens. Matter 64, 2011, p. 075118.
[22] K. Bertoldi, M.C. Boyce, "Mechanically triggered transformations of phononic band gaps in periodic elastomeric structures", Phys. Rev. B: Condens. Matter 77, 2008, p. 052105.